ACS MATERIALS LETTERS

Editors' Choice

www.acsmaterialsletters.org

Flame-Synthesized Zinc Oxide Tetrapods for Photoprotection in Sunscreen Formulations

Ajoa J. Addae,* Jennifer Uyanga, Yogendra Kumar Mishra, Justin Caram, and Paul S. Weiss*

Cite This: https://doi.org/10.1021/acsmaterialslett.5c01351

Read Online

ACCESS | Metrics & More | Article Recommendations | Supporting Information

ABSTRACT: **ZnO nanoparticles are widely used in sunscreen formulations due to their strong light absorption in the ultraviolet (UV) and ease of synthesis. Here, we explore flame-synthesized tetrapod-shaped zinc oxide (ZnO) nanostructured particles (NPs) as UV-absorbing materials for sunscreen formulations. We compare their optical properties to conventional sol−gel-synthesized ZnO NPs. We then tested sunscreen formulations of each and measured and compared their optical, colloidal, and cosmetic properties. Notably, the test sunscreen containing mass-equalized tetrapodal ZnO absorbs in the UVB region and has a sun protection factor (SPF) value comparable to that of sol−gel-synthesized ZnO. Furthermore, colloidal and white cast evaluations of flame-synthesized tetrapodal ZnO demonstrated favorable properties for the storage and usage of sunscreen formulations.**

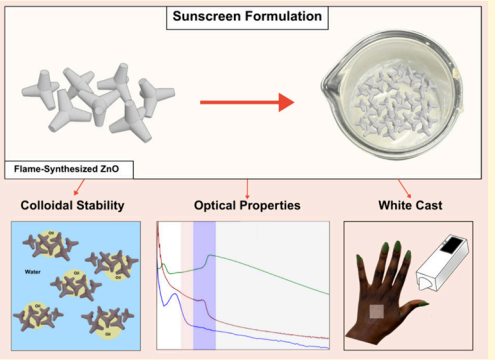

Skin cancers can be induced by exposure to ultraviolet radiation (UVR), leading to DNA mutations through a variety of mechanisms, including direct DNA damage (e.g., formation of thymine dimers) and indirect processes (e.g., reactive oxygen formation and cutaneous inflammatory responses).[1] A notable example of skin cancer onset is due to the photoinduced thymine dimerization in critical protein-coding regions, leading to mutations that can manifest as skin cancers.[2] Daily sunscreen application and reapplication are recommended by dermatologists for preventing UVR-induced damage.[3] The U.S. Food and Drug Administration (FDA) regulates sunscreens as both drugs and cosmetics, but widespread daily sunscreen usage has been limited by challenges around consumer application and user experience.[4,5] Consumers demonstrate preferences for ZnO-based sunscreens over organic sunscreen filters due to their generally recognized safe and effective (GRASE) status.[4,6] The FDA has not approved a new sunscreen filter in over two decades, highlighting the need to advance and to optimize current UV filter materials and their photoprotective properties in sunscreen formulations.[4]

Sunscreens are typically oil-in-water (O/W) or water-in-oil (W/O) emulsions with suspended organic or inorganic UV-absorbing "filters" that absorb UV light (290−400 nm).[4] The resulting sun protection factor (SPF) is determined by measuring the absorbance of UV light when the sunscreen is applied at a film thickness of 2 mg/cm^2.[5,7−9] However, the chemical properties of current UV filters are prone to unfavorable aggregation (inorganic filters) or photodegradation (organic filters), which can cause emulsion instabilities that perturb SPF value.[4,5,10−12] ZnO-based sunscreens, for example, pose significant formulation challenges compared with other UV filters due to the tendency of ZnO to aggregate and to agglomerate, disrupting the formulations' colloidal stability and SPF values.[10−13] Sunscreen functionality is tied to two *interdependent* factors: photoprotection and colloidal stability. Here, we explore flame-transport-synthesized ZnO tetrapod (ZOTeN) particles as promising UV-absorbing alternatives to ZnO particles fabricated by wet chemical methods.[14−16]

ZnO is a semiconductor with strong absorbance in the UV region due to a large direct band gap (~3.37 eV, 368 nm).[16] Despite limitations related to white cast and aggregation in sunscreen formulations addressed here, ZnO remains a suitable material for sunscreen usage due to its broad UVR absorption. The optical properties of ZnO particles, and metal oxide particles generally, relevant for sunscreen absorption are dependent on size, morphology, surface properties, and thus synthetic route.[4,6] We compare these properties when ZnO is obtained by three different synthetic routes (Table 1) and the resulting behaviors of the obtained ZnO in sunscreen suspensions compared to ZOTeN particles.

Received: October 4, 2025
Revised: December 18, 2025
Accepted: December 19, 2025

Table 1. ZnO Particle Types Used in the Present Investigation with Their Synthetic Routes and Properties

ZnO Type	Synthetic Summary	Properties
Sol−gel-synthesized ZnO (SgZnO) particles	Zinc precursor ($Zn(CH_3CO_2)_2{\cdot}2H_2O$) vortexed in water, pH adjusted to 12 with NaOH, vacuum-dried at 50 °C for 12 h	Platelet-shaped ZnO particles, with aggregates ranging in size from 20 to 200 nm
Flame-synthesized ZnO tetrapods (ZOTeN) particles	Zinc precursor (Zn^{2+}) and ethanol heated to 900 °C and vapor flame	Tetrapod-shaped ZnO particle morphologies with arm lengths spanning 10−100 μm
French-process ZnO (FpZnO) particles	Zinc precursor (Zn^{2+}) vaporized at ∼1000 °C, oxidized in oxidation chamber to yield polycrystalline ZnO powder	Platelet-shaped ZnO particles ranging in size from 0.39 to 1.81 μm

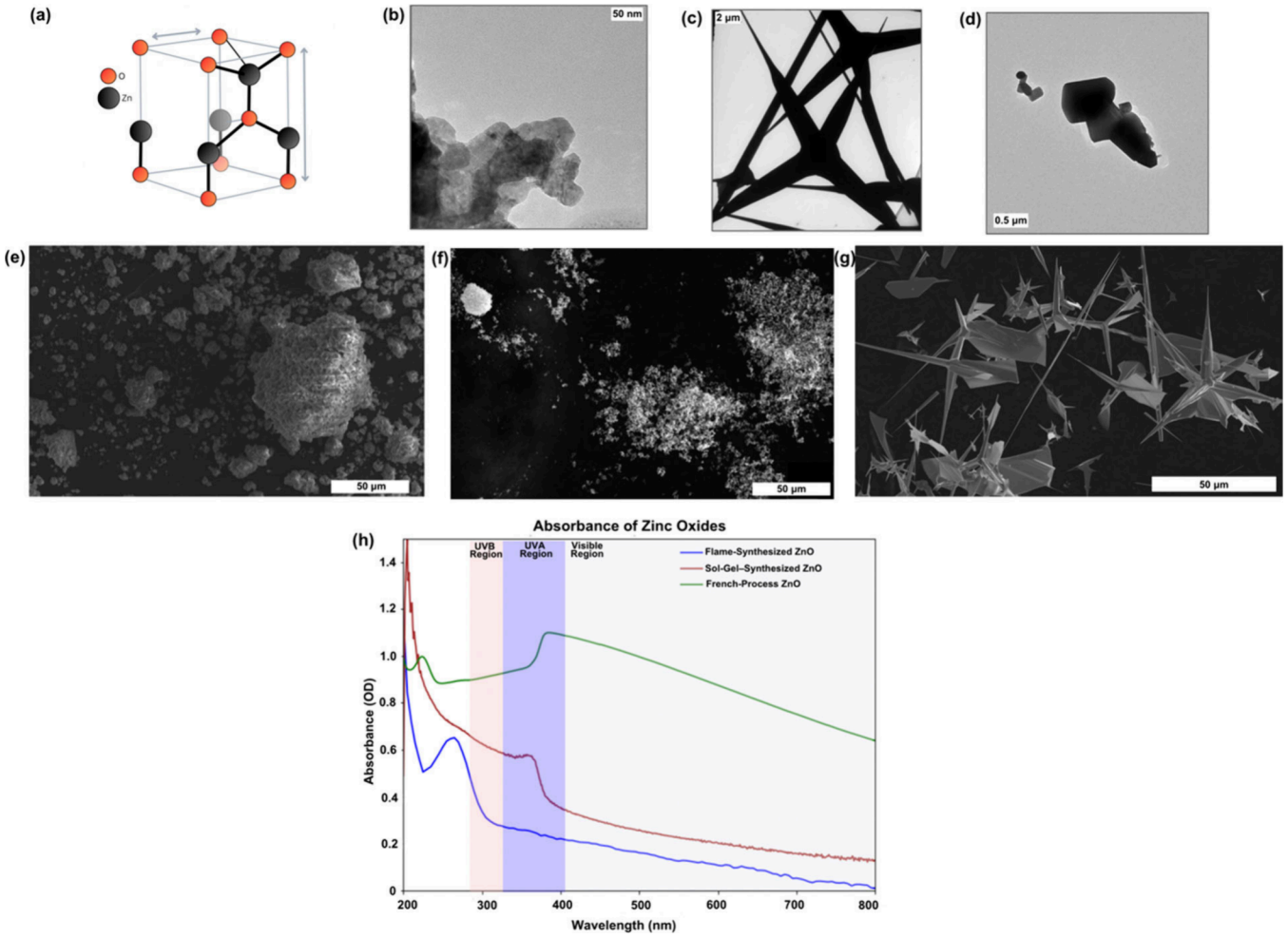

Figure 1. (a) Schematic of anisotropic growth of ZnO within the wurtzite host lattice structure. (b) Transmission electron microscopy image of sol−gel-synthesized ZnO (SgZnO) particles; scale bar 50 μm. (c) Transmission electron microscopy image of flame-synthesized ZnO (ZOTeN) particles; scale bar 2 μm. (d) Transmission electron microscopy image of FpZnO particles; scale bar 0.5 μm. (e) Scanning electron microscopy image of 0.1 g of SgZnO particles; scale bar 50 μm. (f) Scanning electron microscopy image of 0.1 g of FpZnO particles; scale bar 50 μm. (g) Scanning electron microscopy image of 0.1 g of ZOTeN particles; scale bar 50 μm. Absorption spectra of 0.1 g/mL of flame-synthesized ZnO, French-process-synthesized ZnO, and sol−gel-synthesized ZnO in the ultraviolet and visible regions.

van der Waals interactions between ZnO particles in sunscreen formulations can lead to ZnO aggregates and "crowding" of emulsion phases, thereby potentially resulting in phase separation and inconsistent sunscreen photoprotective properties.[8,17,18] Notably, ZnO used in sunscreens is typically surface-treated using silane-based coatings or is suspended within polymeric dispersions that can improve UV absorbance and aesthetic properties.[5,8,19] Moreover, ZnO nanoparticles are of interest for sunscreen formulations due to their efficiency in absorbing UVR, but they demonstrate notable toxicological concerns and aesthetic drawbacks.[4,20,21] In other instances, ZnO has been conjugated with other metal oxides to form composites or utilized alongside other pigments in sunscreen formulations to reduce the white cast associated with ZnO, thereby improving aesthetic properties of the sunscreen.[22−25] Ultimately, careful consideration of the ZnO particle size and morphology used is necessary to obtain suitable photoprotection and cosmetic elegance in sunscreen formulations. These characteristics can be tuned by adjusting synthesis parameters (e.g., temperature, pH), which in turn influence anisotropic growth within the ZnO wurtzite lattice (Figure 1a). Here, we utilize nonsurface-treated ZnO particles fabricated *via* flame-transport synthesis (Table 1) and demonstrate their usage in sunscreen formulations. Sol−gel-synthesized ZnO (SgZnO) particles were chosen as a comparison in our optical and colloidal investigations due to their common and

https://doi.org/10.1021/acsmaterialslett.5c01351
ACS Materials Lett. XXXX, XXX, XXX−XXX

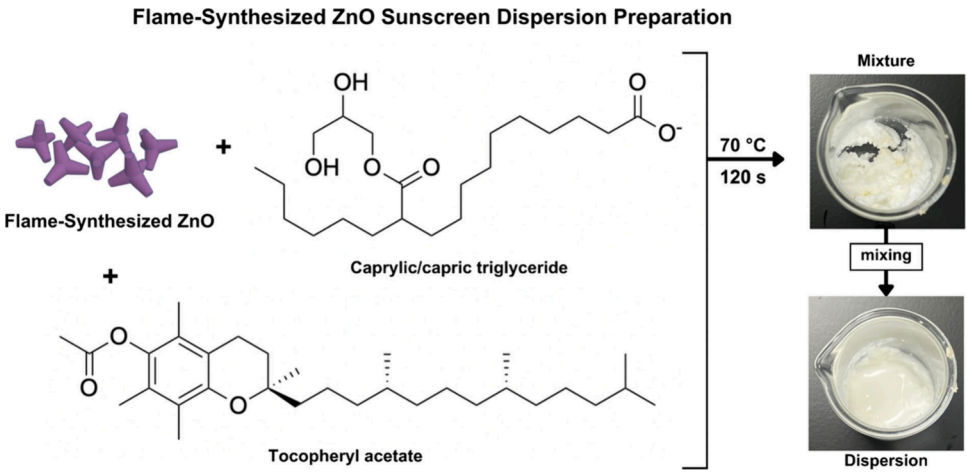

Figure 2. Schematic of preparing flame-synthesized ZnO (ZOTeN) particle dispersions for incorporation into a sunscreen formulation.

previously reported applications in sunscreen formulations. Commercially available French-process ZnO (FpZnO) nanoparticles (Katonah Chemical) were purchased and utilized as an additional control for optical investigations due to their size, synthesis using dry methods, and reported usage in sunscreen formulations.[8,26−28] The ZOTeN particles, which are fabricated using a previously reported flame-transport synthesis method (described further in Supporting Information), have not yet been used in sunscreen applications.[14,15] The ZOTeN particles have four cylindrical "arms", with needlelike ends, radiating from a core to the corners of a tetrahedron (Figure 1). The ZOTeN particles have high surface area-to-volume ratios due to their tetrapod shape, relatively high morphological uniformity, and higher yield compared to other methods of ZnO synthesis (Supporting Information).[29,30] We note that varying temperature and duration of flame-transport synthesis can yield various dimensions of needle sharpness or possible formation of nano-sea urchin and multipod structures.[29,30] Notably, ZOTeN particles are significantly larger than SgZnO and FpZnO particles, potentially allowing for a different format for colloidal suspension. We find that ZOTeN particles demonstrate absorption in the UVB region as well as visible light scattering, and we hypothesize that such properties can be leveraged for sunscreen formulations without relying on surface treatment and coating of ZnO or addition of pigments to the sunscreen formulation.

Here, we report that sunscreens formulated with ZOTeN particles are suitable for use in sunscreens and overcome aesthetic limitations better due to apparent decreases in the visible "white cast". We compare ZnO particles synthesized *via* sol−gel synthesis versus flame transport and French processes; each method reproducibly produces distributions of particles of different size scales and strikingly different morphologies (Figure 1). The SgZnO particles, as well as commercially available ZnO particles, were used as control ZnO particle forms due to their common use in conventional sunscreens and pharmaceutical applications.[8,31−34] After characterizing the ZnO particles, we made standard emollient-based ZnO dispersions to formulate a test sunscreen for each ZnO dispersion (*vide infra*). We evaluate the optical and rheological properties of the sunscreen formulations as well as SPF. Lastly, each test sunscreen was evaluated for "white cast" by applying controlled dosages on various substrates and using colorimetry and absorbance spectroscopy.

CHARACTERIZATION OF ZnO PARTICLES

The ZnO particles from Table 1 were imaged *via* either transmission electron microscopy (TEM) or scanning electron microscopy (SEM) and analyzed using UV/visible spectroscopy (Figure 1) and powder X-ray diffraction (PXRD) (Figure S1). Powder X-ray diffraction showed that all ZnO particles demonstrated wurtzite crystal structures (Figure S1). The SgZnO particles displayed nonuniform morphologies and were 20 to 100 nm in length. We note that SgZnO and FpZnO particles aggregate and agglomerate with individual particles in contact with one another, as observed in the TEM micrographs (Figure 1). The ZOTeN particles were the largest ZnO particles in size and surface area, as also shown in TEM and SEM micrographs. When measured using PXRD, ZOTeN particles displayed higher intensity in crystallinity than both SgZnO and FpZnO particles (Supporting Information Figure S1). We attribute the higher crystallinity of ZOTeN particles to their larger sizes and greater purity compared to SgZnO particles, prepared using wet methods.[14,15]

Because sunscreen formulations require absorption in the UVA (320−400 nm) and UVB (290−320 nm) regions, UV/visible spectroscopy was used to analyze the absorbance of 0.1 mg/mL of each ZnO particle type in both the UV region (290−400 nm) and visible region (400−800 nm).[35] The SgZnO and FpZnO particles were solubilized in ethanol, and ZOTeN particles were solubilized in 0.01 M HCl due to their poor solubility in ethanol. The visible region was measured to evaluate scattering, which is a possible indication of white cast caused by ZnO when present in a sunscreen formulation.[4,36] We note that solubility, accessible surface area of varying ZnO morphologies, and domination of scattering in the visible region by ZnO can influence UV/visible absorption spectra characteristics. The SgZnO particles displayed an exciton peak at *ca.* 370 nm (Figure 1f), corresponding to the maximum absorption in the UVA region, consistent the material's wide band gap previously reported, of ∼3.37 eV.[18,37] The FpZnO displayed the highest absorbance of the ZnO types, with an absorbance peak at 395 nm, likely due to a smaller particle size, and a band gap of 3.14 eV. The ZOTeN particles have an absorption peak at 265 nm, absorb in the UVC and UVB regions, and possess a larger band gap of 4.68 eV.[38] The

https://doi.org/10.1021/acsmaterialslett.5c01351
ACS Materials Lett. XXXX, XXX, XXX−XXX

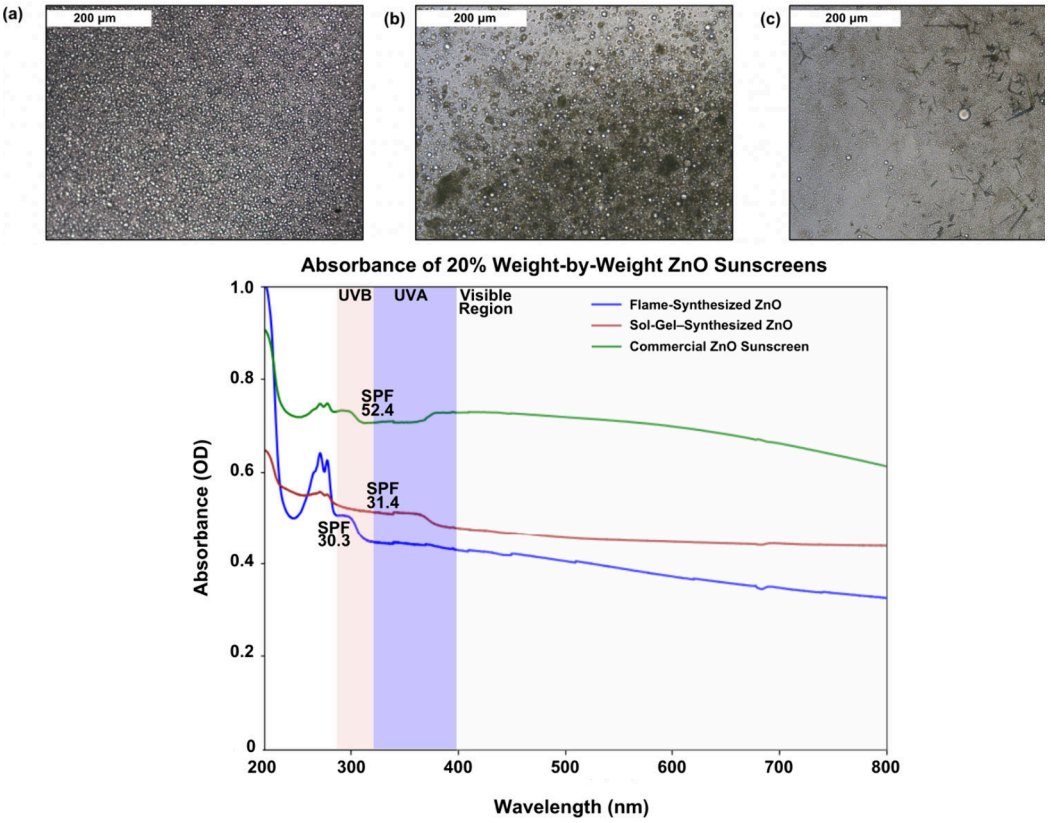

Figure 3. (a) Light microscope image of a 1:50 dilution of test formulation without ZnO in water, with scale bars of 200 μm. (b) Light microscope image of a 1:50 dilution of test formulation with sol−gel-synthesized ZnO (SgZnO) particles in water, with scale bars of 200 μm. (c) Light micrograph of a 1:50 dilution of test formulation with flame-synthesized ZnO (ZOTeN) particles in water, with scale bars of 200 μm. (d) Absorbance of ZOTeN particle sunscreen test formulation, SgZnO particle sunscreen test formulation, and FpZnO particle sunscreen test formulation.

ZOTeN particles showed less scattering in the visible region in comparison to SgZnO and FpZnO particles, which suggests less protection from UVA wavelengths.[4]

FORMULATION OF SUNSCREEN DISPERSIONS AND TEST EMULSIONS

When ZnO is added directly to a sunscreen formulation without predispersion in a medium such as a silicone-based dispersant or emollient, it is prone to aggregate within the final formulation. To minimize this aggregation, formulators use "dispersions" of ZnO or TiO_2, in which particles are precoated in emollients for incorporation into sunscreen formulations (Figure 2). These dispersions improve incorporation into colloidal suspensions and help maintain emulsion stability by reducing particle-induced droplet disruption.[8,39,40] To compare the optical characteristics of sunscreens containing ZOTeN versus SgZnO particles, dispersions were prepared containing ZOTeN particles, caprylic/capric triglyceride, and tocopheryl acetate. Caprylic/capric triglyceride and tocopheryl acetate were chosen due to their cost, wide availability, and cosmetic benefits. Furthermore, caprylic/capric triglyceride is an effective emollient used in sunscreen formulations due to its ability to spread favorably on the skin's surface, which is essential for sunscreen film formation.[5,13,41] A 50 g ZnO particle dispersion was prepared with caprylic/capric triglyceride and tocopheryl acetate, then incorporated into a prepared dispersed phase, resulting in a sunscreen "test" formulation with 20% weight by weight composition of ZOTeN particles (Supporting Information). The final formulations each have the following International Nomenclature of Cosmetic Ingredients (INCI) declaration: Water (Aqua), Caprylic/Capric Triglyceride, Zinc Oxide, Cetearyl Alcohol, Polysorbate 60, Tocopherol, Phenoxyethanol, Cetearyl Glucoside, Hydroxyethylcellulose, Ethylhexylglycerin, Glucose. We note that each material in the present sunscreen formulations carry GRASE status by the US Food and Drug Administration. The same process was repeated with SgZnO and FpZnO particles to create comparison sunscreens for optical and colloidal investigations.

SUNSCREEN FORMULATION CHARACTERIZATION

A 1:50 dilution of each test sunscreen was prepared by suspending 1 g of sunscreen in 50 mL of water; the mixture was then visualized under a light microscope (Nikon EV4500). An additional formulation similar to the test sunscreens was created, without ZnO, to provide a "reference" emulsion when visualized under light microscopy (INCI: Water (Aqua), Caprylic/Capric Triglyceride, Cetearyl Alcohol, Polysorbate 60, Tocopherol, Phenoxyethanol, Cetearyl Glucoside, Hydroxyethylcellulose, Ethylhexylglycerin, Glucose) (Figure 3a). The sunscreen formulations were visualized using light microscopy to measure the aggregation and particle size of ZnO candidates when suspended in emulsions. Additional microscope images of the sunscreen formulations were taken using scanning electron microscopy (SEM) (Supporting Information Figure S2) to visualize interlocking of ZnO aggregates formed by

https://doi.org/10.1021/acsmaterialslett.5c01351
ACS Materials Lett. XXXX, XXX, XXX−XXX

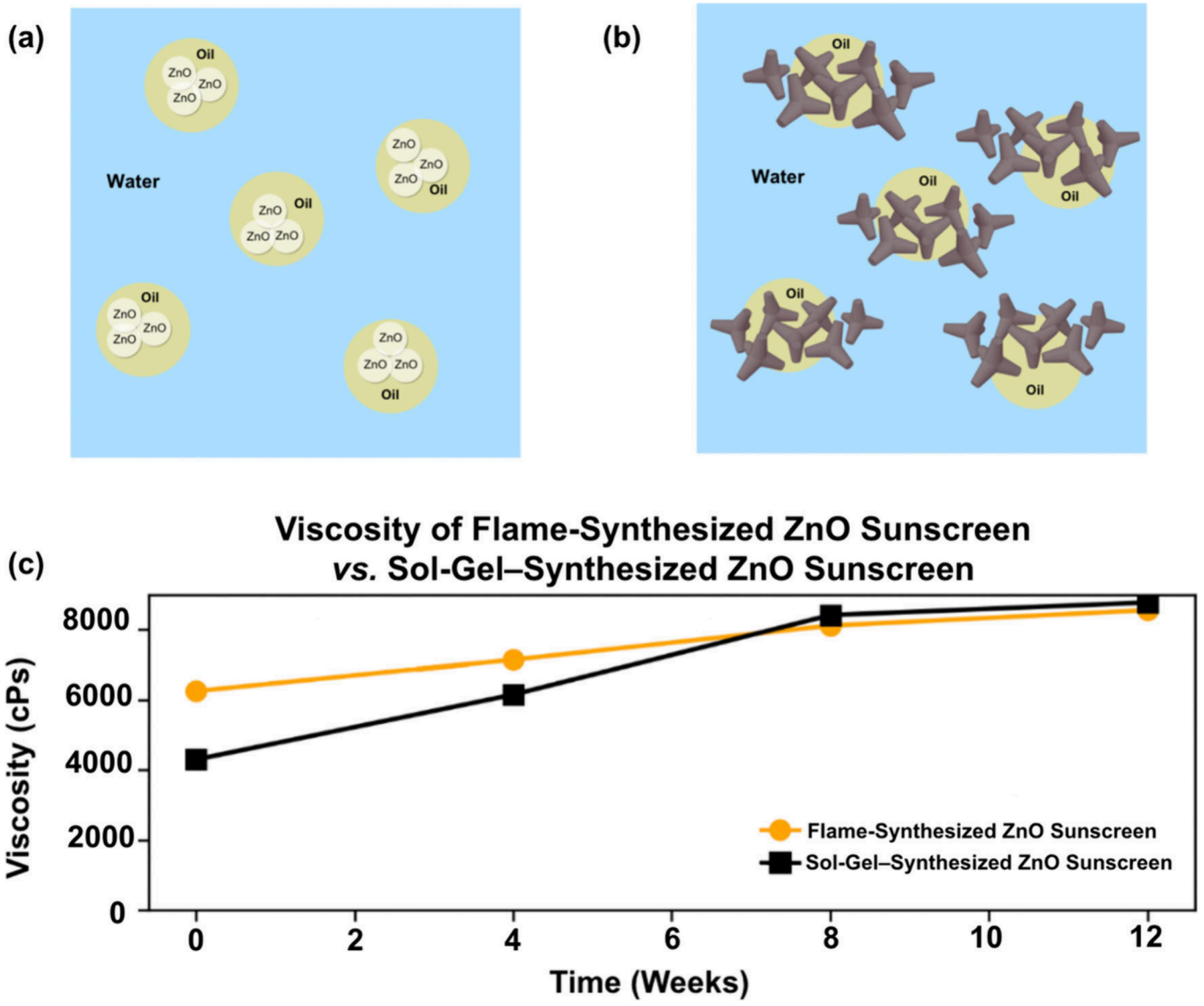

Figure 4. (a) Schematic of oil-in-water emulsions containing sol–gel-synthesized ZnO and (b) flame-synthesized ZnO. (c) Viscosity measurements of flame-synthesized ZnO sunscreen and sol–gel-synthesized ZnO sunscreen over 12 weeks at 25 °C.

ZOTeN particles, versus nonuniform ZnO aggregates formed by SgZnO particles. The sunscreen formulations with SgZnO particles displayed comparatively more ZnO aggregates, indicative of potential disruption to the colloidal stability of the emulsion (Figure 3b,c).

The sunscreens' absorption and transmission spectra were measured using a Shimadzu UV-2550 UV/visible spectrophotometer, with 2 mg/cm^2 of each sunscreen sample applied to the inner surface of a quartz cuvette. *In vivo* determination of SPF remains the standard method of determining SPF, but it is not feasible for facile benchtop sunscreen measurements. To correlate to methods used in *in vivo* determination of SPF, a thin-film approach was taken where a 2 mg/cm^2 sample of sunscreen was weighed using an analytical balance and uniformly spread onto one side of the inner transparent cuvette surface using a spatula. A 2 mg/cm^2 film deposition was achieved because the optical window of the quartz cuvette is 1 cm. The film was placed in a UV/visible spectrometer cuvette holder to measure the absorbance of the SgZnO, FpZnO, and ZOTeN particle sunscreens in the UV and visible regions (Figure 3d,e). Measuring absorption using thin films of sunscreen samples was selected over aqueous, solvent-based spectroscopic methods due to closer representation of the *in vivo* determination of SPF on human skin.[5,10,42]

Notably, all light microscope images displayed that ZOTeN particles in the test sunscreens were larger than the oil droplets dispersed in the continuous phase (Figure 4a schematic). Furthermore, the formulation containing ZOTeN particles visually displayed smaller oil droplets when photographed under a light microscope at the same scale as the formulation containing SgZnO particles (Figure 3).

To measure how the prepared sunscreen formulations' stabilities performed over extended time periods, the test sunscreen emulsions were incubated in sealed plastic jars at 25 °C for 12 weeks. Viscosity measurements in centipoise (cPs) using a Brookfield DV3T Viscometer were recorded at baseline, 2, 4, 8, 10, and 12 weeks. Viscosity was evaluated because it influences spreadability in all sunscreen systems, and agglomeration and phase separation in inorganic sunscreen systems are indicated by decrease in viscosity over time (Figure 4c).[18,43] The viscosity of the sunscreen containing SgZnO particles nearly doubled between weeks 0 (4300 cPs) and 12

https://doi.org/10.1021/acsmaterialslett.5c01351
ACS Materials Lett. XXXX, XXX, XXX−XXX

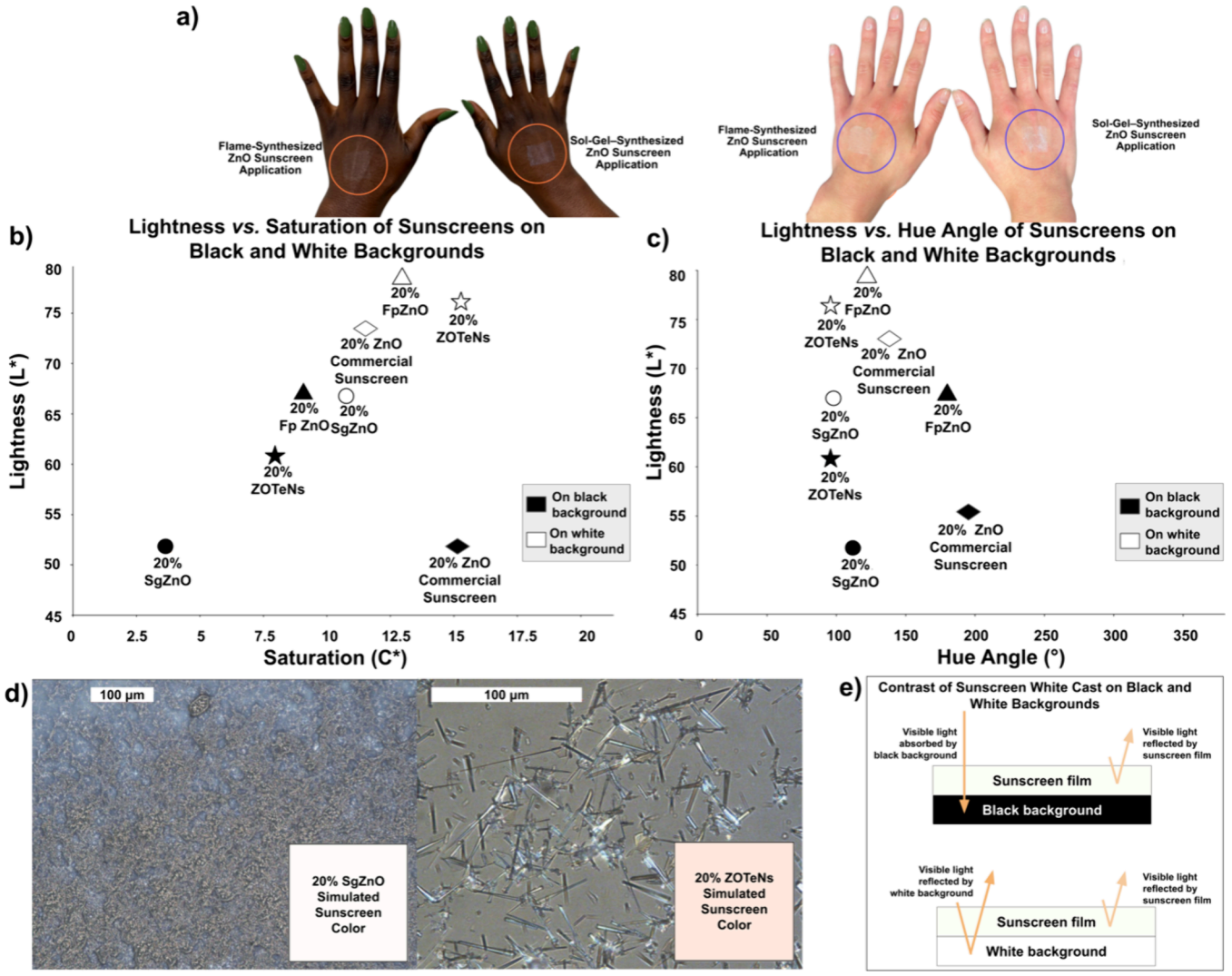

Figure 5. (a) Image of flame-synthesized (ZOTeN) particle-based sunscreen and sol−gel-synthesized (SgZnO) particle-based sunscreen application on hands categorized as (left) Fitzpatrick Skin Type 6 (darker tone) and image of ZOTeN particles and SgZnO particles application on hands categorized as (right) Fitzpatrick Skin Type 2 (lighter tone). (b) Lightness versus saturation of 20% w/w SgZnO particle-based sunscreen, 20% w/w ZOTeN particle-based sunscreen, 20% w/w FpZnO particle-based sunscreen, and 20% w/w ZnO commercial sunscreen on black and white backgrounds. (c) Lightness versus hue of 20% w/w sol−gel-synthesized ZnO (SgZnO) particle sunscreen, 20% w/w flame-synthesized (ZOTeN) particle sunscreen, 20% w/w FpZnO particle-based sunscreen, and 20% w/w ZnO commercial sunscreen particle sunscreen on black and white backgrounds. (d) Light microscope image of 1 g of 20% w/w SgZnO particle sunscreen with scale bars of 100 μm with UV/visible spectrum-simulated color swatch superimposed in the bottom right corner (left) and 1 g of 20% w/w ZOTeN particle sunscreen with scale bars of 100 μm with UV/Visible spectrum-simulated color swatch superimposed in the bottom right corner (right). (e) Diagram depicting contrast of sunscreen white cast on absolute black and white backgrounds.

(8600 cPs), whereas the viscosity of the sunscreen containing ZOTeN particles increased steadily between weeks 0 (6250 cPs) and 12 (8780 cPs) (Figure 4b), with a 40.5% increase. The viscosity measurements of the sunscreen containing ZOTeN particles are higher than SgZnO particles sunscreen at week 0 but are similar to those of SgZnO particles sunscreens at weeks 8 through 12, suggesting improved emulsion stability characteristics of the ZOTeNs particles sunscreen. Notably, the sunscreen containing ZOTeN particles was more viscous at week 0, which we tentatively attribute to the porous networks formed by ZOTeN particles (Figure S2) in the sunscreen emulsions.

days 0, 7, 14, and 21

To evaluate stability further, centrifugal aging was performed on each sunscreen formulation on days 0, 7, 14, and 21 after storage at room temperature (Supporting Information).

We use the Mansur equation (eq 1) to evaluate the SPF value of the formulated sunscreens using the measured absorbance spectrum values (Figure 3d):

$$SPF = CF \sum_{290}^{320} EE(\lambda) \cdot I(\lambda) \cdot Abs(\lambda) \quad (1)$$

where CF is a correction factor of 10, $EE(\lambda)$ is the skin reddening minimal erythema dose caused by wavelength λ, $I(\lambda)$ is the solar intensity at a specific wavelength, and $Abs(\lambda)$ is the spectrophotometric absorbance at wavelength λ.[7] The calculated SPF values using the Mansur equation are 30.3 for the flame-synthesized ZnO sunscreen, 31.4 for the sol−gel-synthesized ZnO sunscreen, and 52.4 for the ZnO made by French process, at the same weight by weight percentage of ZnO. The UV/vis spectra of each sunscreen formulation

https://doi.org/10.1021/acsmaterialslett.5c01351
ACS Materials Lett. XXXX, XXX, XXX−XXX

exhibit absorbance features characteristic of ZnO in addition to scattering contributions in the visible region, which are most evident by FpZnO sunscreen.

COLORIMETRIC EVALUATION OF SUNSCREEN FORMULATIONS

To evaluate the "white cast" potential of the sunscreen formulations, a 3 × 3 cm square (9 cm^2) was marked on the skin using a ruler to define the region for sunscreen application. To display "white cast" contrast on lighter and darker skin tones, images of Fitzpatrick Skin Type 6 and Fitzpatrick Skin Type 2 human hands were taken following an application dosage of 2 mg/cm^2 to marked areas on the dorsum of the hands. The sunscreen was evenly spread within the marked region using a spatula to provide uniform coverage (Figure 5a). The application region was left to dry for 15 min and photographed in standard lighting conditions.

To measure the color of the sunscreen formulations and their relationship to contrast, we applied 2 mg of each sunscreen (20% w/w SgZnO particles, 20% w/w FpZnO particles, or 20% w/w ZOTeN particles) and a commercial sunscreen formulation containing 20% ZnO (TiZO) for further comparison onto 2 cm squares of black or white Kodak Portra paper, which were weighed for accuracy. Black and white paper colors were chosen to simulate the darkest and lightest possible color application backgrounds, respectively. A hand-held colorimeter (Delfin Technologies) was used to measure color values a* which represents the position on the green (−) to red (+) axis, L* which measures the lightness of the color, and b* represents the position on the blue (−) to yellow (+) axis.[44−46] Each measurement was performed five times, and the average values and their standard deviations are reported (Figure 5b,c).

Colorimetry measurements were converted to calculate color saturation and hue, using eqs 2 and 3:

$$C^* = \sqrt{a^{*2} + b^{*2}} \tag{2}$$

where C* is the distance from the origin in the a*-b* plane, representing color saturation (i.e., "chroma") (eq 2). We define color saturation as the intensity of a color. Colors with C* = 0 appear perceptually neutral gray, and saturation increases as C* rises with greater distance from the neutral axis:

$$h^\circ = arctan\left(\frac{b^*}{a^*}\right) \tag{3}$$

where h is the hue angle in degrees (eq 3). A hue angle of 90° is associated with yellow, 180° is associated with green, and 270° is associated with blue.

Using the measured L*, a*, and b* values, the sunscreens' apparent colors on white and black backgrounds were approximated by plotting lightness versus saturation (Figure 5b) and lightness versus hue angle (Figure 5c) to determine the contrast of "white cast" on white and black backgrounds (Table S1).[47,48]

The standard deviation of hue on black paper reflects that both a* and b* values are closer to zero in magnitude than on white paper; in such cases, minor numerical variations in a* or b* can produce large apparent changes in hue angle without perceptible shifts in color.[45,46] The reported colorimetry measurements (Table S1, Figure 5d) indicate that the 20% w/w ZOTeN particles sunscreen appears as a warm-yellow hue with moderate saturation on black backgrounds and a pure yellow hue with moderate to high saturation on white backgrounds. The 20% FpZnO sunscreen exhibited the highest lightness value, C* and hue angle values corresponding to cooler yellow tints on white backgrounds, and bluish-gray films on black backgrounds. The 20% SgZnO's C* and hue angle values correspond to warm pale yellows on white backgrounds and desaturated white-gray films on black backgrounds with little hue. The TiZO sunscreen demonstrated neutral yellow-green with moderate saturation on white backgrounds and strong bluish-gray tones on dark backgrounds with comparatively lower lightness values than the other sunscreens. Although the sunscreen with ZOTeN particles exhibited higher lightness (L*) values than most of the ZnO formulations, it also presented higher saturation (C*); thus, chroma, lightness, and hue should be considered together when assessing reduction in visible white cast. Importantly, unlike the test formulations, the TiZO sunscreen formulation contains emollients and film formers that aid in aesthetic improvements of the sunscreen. We note that the color black is perceived by the human eye when little to no visible light is reflected from a surface, whereas the color white is perceived by the human eye when visible light is reflected equally. Therefore, the visible "white cast" of ZnO sunscreens is exacerbated by perceptible contrast when sunscreens are applied to darker backgrounds that absorb visible light, while the sunscreen reflects visible light, whereas lighter backgrounds reflect visible light in addition to the sunscreen (Figure 5e).

The simulated colors of the sunscreens were displayed in comparison to light microscope images of the sunscreens (Figure 5c and Supporting Information).

In summary, we fabricated tetrapod-shaped ZnO particles *via* flame synthesis and demonstrated their UV-absorption activity, sunscreen formulation emulsion stability, and cosmetic advantages in sunscreen formulations due to diminished white cast. We present a facile method to evaluate the colorimetric properties of sunscreen formulations and demonstrate that FpZnO particles with comparatively higher UV absorbance than SgZnO particles and ZOTeN particles result in higher white cast on darker substrates. Our color simulation data suggest that perceptible "white cast" from ZnO-based sunscreen formulations is influenced by the warmth of the sunscreen's hue and contrast caused by the applied surface's color. While our color simulation methods are limited to absolute black and white backgrounds, we note that these methods can be extended across various skin tones in future work for human-like color matching. Nevertheless, ZOTeN particles demonstrated favorable color matching closer to human-like skin tones when compared to all sunscreens evaluated. Our work highlights the relationship between ZnO particle synthesis and morphology and the impacts of the properties of the synthesized ZnO on UVA and UVB absorption in sunscreen formulations. We anticipate that these findings can improve the aesthetic and stability-related drawbacks of ZnO-based sunscreens.

ASSOCIATED CONTENT

Supporting Information

The Supporting Information is available free of charge at https://pubs.acs.org/doi/10.1021/acsmaterialslett.5c01351.

X-ray diffraction data of ZnO particles and SEM and calculated values of saturation and hue. Methods of

https://doi.org/10.1021/acsmaterialslett.5c01351
ACS Materials Lett. XXXX, XXX, XXX−XXX

synthesis and Python processing of colors. Centrifugal aging data of sunscreens. (PDF)

AUTHOR INFORMATION

Corresponding Authors

Ajoa J. Addae − *Department of Chemistry and Biochemistry, University of California Los Angeles, Los Angeles, California 90095, United States; California NanoSystems Institute, University of California Los Angeles, Los Angeles, California 90095, United States*; Email: ajoaaddae@gmail.com

Paul S. Weiss − *Department of Chemistry and Biochemistry, University of California Los Angeles, Los Angeles, California 90095, United States; California NanoSystems Institute and Department of Materials Science and Engineering, University of California Los Angeles, Los Angeles, California 90095, United States; Department of Bioengineering, University of California, Los Angeles, Los Angeles, California 90095, United States;* orcid.org/0000-0001-5527-6248; Email: psw@cnsi.ucla.edu

Authors

Jennifer Uyanga − *Department of Chemistry and Biochemistry, University of California Los Angeles, Los Angeles, California 90095, United States*

Yogendra Kumar Mishra − *Smart Materials, NanoSYD, Mads Clausen Institute, University of Southern Denmark, 6400 Sønderborg, Denmark;* orcid.org/0000-0002-8786-9379

Justin Caram − *Department of Chemistry and Biochemistry, University of California Los Angeles, Los Angeles, California 90095, United States;* orcid.org/0000-0001-5126-3829

Complete contact information is available at: https://pubs.acs.org/10.1021/acsmaterialslett.5c01351

Author Contributions

CRediT: **Ajoa J Addae** conceptualization, data curation, formal analysis, investigation, methodology, validation, visualization, writing - original draft, writing - review & editing; **Jennifer Uyanga** formal analysis, investigation, methodology, validation, visualization, writing - original draft, writing - review & editing; **Yogendra Kumar Mishra** funding acquisition, investigation, methodology, project administration, resources, supervision, validation, visualization, writing - original draft, writing - review & editing; **Justin Ryan Caram** conceptualization, formal analysis, funding acquisition, investigation, methodology, project administration, resources, supervision, validation, visualization, writing - original draft, writing - review & editing; **Paul S. Weiss** conceptualization, data curation, formal analysis, funding acquisition, methodology, project administration, resources, supervision, writing - original draft, writing - review & editing.

Notes

The authors declare the following competing financial interest(s): A.J.A., P.S.W., and Y.K.M. have patent applications related to this work.

ACKNOWLEDGMENTS

The authors thank the Challenge Initiative at UCLA and Sigma Xi IFoRE Grant-in-Aid for support. A.J.A. thanks the National Science Foundation for graduate fellowship support (Grant DGE-2034835 and DGE-2444110). Y.K.M. acknowledges NANOCHEM (national infrastructure UFM 5229-00010B, NANOCHEM, Denmark) and Fabrikant Mads Clausen Fonden Denmark for a Tetrapod Upscaling Grant. We thank the California NanoSystems Institute Core Voucher program for supporting measurements. The authors thank Antonio Macias, Jr. for assistance with X-ray diffraction, Alexandra Wright for images of her hands, Daniel Bilezikian for assistance with SEM, Elijah Cook for assistance with TEM, Bradley Kroes for assistance with ball milling, and Dr. Krzysztof Konieczny and Prof. Thomas Mason for helpful discussions.

REFERENCES

(1) Taylor, J. S. Unraveling the Molecular Pathway from Sunlight to Skin Cancer. *Acc. Chem. Res.* **1994**, *27*, 76−82.

(2) Rastogi, R. P.; Richa; Kumar, A.; Tyagi, M. B.; Sinha, R. P. Molecular Mechanisms of Ultraviolet Radiation-Induced DNA Damage and Repair. *J. Nucleic Acids* **2010**, *2010*, 592980.

(3) Neale, R.; Williams, G.; Green, A. Application Patterns among Participants Randomized to Daily Sunscreen Use in a Skin Cancer Prevention Trial. *Arch. Dermatol.* **2002**, *138*, 1319−1325.

(4) Addae, A. J.; Weiss, P. S. Standardizing the White Cast Potential of Sunscreens with Metal Oxide Ultraviolet Filters. *Acc. Mater. Res.* **2024**, *5*, 392−399.

(5) Addae, A. J.; Uyanga, J.; Chifamba, J.; Weiss, P. S. Advances in Enhancing Photoprotection of Sunscreens Using Hydrocarbon Film Formers and Carbon Nanomaterials. *Adv. Drug Delivery Rev.* **2025**, *222*, 115607.

(6) Xu, S.; Kwa, M.; Agarwal, A.; Rademaker, A.; Kundu, R. V. Sunscreen Product Performance and Other Determinants of Consumer Preferences. *JAMA Dermatol.* **2016**, *152*, 920−927.

(7) Herzog, B.; Schultheiss, A.; Giesinger, J. On the Validity of Beer-Lambert Law and Its Significance for Sunscreens. *Photochem. Photobiol.* **2018**, *94*, 384−389.

(8) Lowe, N. J.; Shaath, N. A.; Pathak, M. A. *Sunscreens: Development: Evaluation, and Regulatory Aspects*, 2nd ed.; Marcel Dekker, Inc., 1997.

(9) Khunkitti, W.; Satthanakul, P.; Waranuch, N.; Pitaksuteepong, T.; Kitikhun, P. Method for Screening Sunscreen Cream Formulations by Determination of *in Vitro* SPF and PA Values Using UV Transmission Spectroscopy and Texture Profile Analysis. *J. Cosmet. Sci.* **2014**, *65*, 147−159.

(10) Binks, B. P.; Brown, J.; Fletcher, P. D. I.; Johnson, A. J.; Marinopoulos, I.; Crowther, J. M.; Thompson, M. A. Evaporation of Sunscreen Films: How the UV Protection Properties Change. *ACS Appl. Mater. Interfaces* **2016**, *8*, 13270−13281.

(11) Stiller, S.; Gers-Barlag, H.; Lergenmueller, M.; Pflücker, F.; Schulz, J.; Wittern, K. P.; Daniels, R. Investigation of the Stability in Emulsions Stabilized with Different Surface Modified Titanium Dioxides. *Colloids Surf. Physicochem. Eng. Asp.* **2004**, *232*, 261−267.

(12) Yeon, J. Y.; Seo, J. M.; Kim, T. H.; Shim, J. G. Emulsion Stability of Low Viscosity W/O Emulsion and Application of Inorganic Sunscreen Agents. *J. Korean Appl. Sci. Technol.* **2018**, *35*, 985−1001.

(13) Chao, C.; Génot, C.; Rodriguez, C.; Magniez, H.; Lacourt, S.; Fievez, A.; Len, C.; Pezron, I.; Luart, D.; van Hecke, E. Emollients for Cosmetic Formulations: Towards Relationships between Physico-Chemical Properties and Sensory Perceptions. *Colloids Surf. Physicochem. Eng. Asp.* **2018**, *536*, 156−164.

(14) Mishra, Y. K.; Adelung, R. ZnO Tetrapod Materials for Functional Applications. *Mater. Today* **2018**, *21*, 631−651.

(15) Mishra, Y. K.; Kaps, S.; Schuchardt, A.; Paulowicz, I.; Jin, X.; Gedamu, D.; Freitag, S.; Claus, M.; Wille, S.; Kovalev, A.; Gorb, S. N.; Adelung, R. Fabrication of Macroscopically Flexible and Highly Porous 3D Semiconductor Networks from Interpenetrating Nanostructures by a Simple Flame Transport Approach. *Part. Part. Syst. Charact.* **2013**, *30*, 775−783.

(16) Klingshirn, C. ZnO: Material, Physics and Applications. *ChemPhysChem* **2007**, *8*, 782−803.

(17) Lu, P. J.; Fang, S. W.; Cheng, W. L.; Huang, S. C.; Huang, M. C.; Cheng, H. F. Characterization of Titanium Dioxide and Zinc Oxide Nanoparticles in Sunscreen Powder by Comparing Different Measurement Methods. *J. Food Drug Anal.* **2018**, *26*, 1192−1200.
(18) Saito, G. P.; Bizari, M.; Cebim, M. A.; Correa, M. A.; Jafelicci Junior, M.; Davolos, M. R. Study of the Colloidal Stability and Optical Properties of Sunscreen Creams. *Eclet. Quim. J.* **2019**, *44*, 26−36.
(19) Faure, B.; Salazar-Alvarez, G.; Ahniyaz, A.; Villaluenga, I.; Berriozabal, G.; De Miguel, Y. R.; Bergström, L. Dispersion and Surface Functionalization of Oxide Nanoparticles for Transparent Photocatalytic and UV-Protecting Coatings and Sunscreens. *Sci. Technol. Adv. Mater.* **2013**, *14*, 023001.
(20) Paiva, J. P.; Diniz, R. R.; Leitão, A. C.; Cabral, L. M.; Fortunato, R. S.; Santos, B. A. M. C.; de Pádula, M. Insights and Controversies on Sunscreen Safety. *Crit. Rev. Toxicol.* **2020**, *50*, 707−723.
(21) Schilling, K.; Bradford, B.; Castelli, D.; Dufour, E.; Nash, J. F.; Pape, W.; Schulte, S.; Tooley, I.; van den Bosch, J.; Schellauf, F. Human Safety Review of "Nano" Titanium Dioxide and Zinc Oxide. *Photochem. Photobiol. Sci.* **2010**, *9*, 495−509.
(22) Aditya, A.; Chattopadhyay, S.; Gupta, N.; Alam, S.; Veedu, A. P.; Pal, M.; Singh, A.; Santhiya, D.; Ansari, K. M.; Ganguli, M. ZnO Nanoparticles Modified with an Amphipathic Peptide Show Improved Photoprotection in Skin. *ACS Appl. Mater. Interfaces* **2019**, *11*, 56−72.
(23) Abadi, P. G.-S.; Shirazi, F. H.; Joshaghani, M.; Moghimi, H. R. Ag+-Promoted Zinc Oxide [Zn(O):Ag]: A Novel Structure for Safe Protection of Human Skin against UVA Radiation. *Toxicol. In Vitro* **2018**, *50*, 318−327.
(24) Khanam, B. R.; Nidhi, M. K. J.; Nagaraja, H.; Manjunatha, T.; Angadi, B.; Uma Reddy, B.; Udaykumar, K. Physicochemical and Therapeutic Studies of Microwave-Synthesized ZnO and Cr-Doped ZnO Nanoparticles for Biomedical Applications. *Inorg. Chem. Commun.* **2024**, *170*, 113454.
(25) Bouie, A.; Baki, G. Iron Oxides and Ultramarine Blue in Inorganic Sunscreens for Dark Skin. *J. Cosmet. Sci.* **2025**, *76*, 123−139.
(26) Dipak, Nipane; Thakare, S. R.; Khati, N. T. ZnO Nanoparticle by Sol-Gel and Its UV Application in Cosmetics Formulation. *Int. J. Knowl. Eng.* **2012**, *3*, 168−169.
(27) Al-luhaibi, A. A.; Sendi, R. K. Synthesis, Potential of Hydrogen Activity, Biological and Chemical Stability of Zinc Oxide Nanoparticle Preparation by Sol-Gel: A Review. *J. Radiat. Res. Appl. Sci.* **2022**, *15*, 238−254.
(28) Hong, H. S. Current Status of Zinc Oxide Nanopowder Manufacturing Technology for UV Filters. *Korean J. Mater. Res.* **2025**, *35*, 167−174.
(29) Mishra, Y. K.; Modi, G.; Cretu, V.; Postica, V.; Lupan, O.; Reimer, T.; Paulowicz, I.; Hrkac, V.; Benecke, W.; Kienle, L.; Adelung, R. Direct Growth of Freestanding ZnO Tetrapod Networks for Multifunctional Applications in Photocatalysis, UV Photodetection, and Gas Sensing. *ACS Appl. Mater. Interfaces* **2015**, *7*, 14303−14316.
(30) Modi, G. Zinc Oxide Tetrapod: A Morphology with Multifunctional Applications. *Adv. Nat. Sci.: Nanosci. Nanotechnol.* **2015**, *6*, 033002.
(31) Mueen, R.; Lerch, M.; Cheng, Z.; Konstantinov, K. Na-Doped ZnO UV Filters with Reduced Photocatalytic Activity for Sunscreen Applications. *J. Mater. Sci.* **2020**, *55*, 2772−2786.
(32) Chegeni, M.; Pour, S. K.; Faraji Dizaji, B. Synthesis and Characterization of Novel Antibacterial Sol-Gel Derived TiO_2/Zn2TiO_4/Ag Nanocomposite as an Active Agent in Sunscreens. *Ceram. Int.* **2019**, *45*, 24413−24418.
(33) Hasnidawani, J. N.; Azlina, H. N.; Norita, H.; Bonnia, N. N.; Ratim, S.; Ali, E. S. Synthesis of ZnO Nanostructures Using Sol-Gel Method. *Procedia Chem.* **2016**, *19*, 211−216.
(34) Elbrolesy, A.; Elhussiny, F. A.; Abdou, Y.; Morsy, R. Facile Synthesis and Biophysical Characterization of Novel Zinc Oxide/Fe_3O_4 Hybrid Nanocomposite as a Potentially Active Agent in Sunscreens. *Arab. J. Sci. Eng.* **2024**, *49*, 1083−1093.
(35) Aikens, P. Formulation of Sunscreens in the United States. In *Handbook of Formulating Dermal Applications*; John Wiley & Sons, Ltd, 2016; pp 589−609.
(36) Egerton, T. A.; Tooley, I. R. UV Absorption and Scattering Properties of Inorganic-Based Sunscreens. *Int. J. Cosmet. Sci.* **2012**, *34*, 117−122.
(37) Arif, A.; Belahssen, O.; Gareh, S.; Benramache, S. The Calculation of Band Gap Energy in Zinc Oxide Films. *J. Semicond.* **2015**, *36*, 013001−013006.
(38) Marín, E.; Calderón, A. Conversion of Wavelength and Energy Scales and the Analysis of Optical Emission Spectra. *J. Phys. Chem. Lett.* **2022**, *13*, 8376−8379.
(39) Catalano, R.; Masion, A.; Ziarelli, F.; Slomberg, D.; Laisney, J.; Unrine, J. M.; Campos, A.; Labille, J. Optimizing the Dispersion of Nanoparticulate TiO_2-Based UV Filters in a Non-Polar Medium Used in Sunscreen Formulations - The Roles of Surfactants and Particle Coatings. *Colloids Surf. Physicochem. Eng. Asp.* **2020**, *599*, 124792.
(40) Labille, J.; Feng, J.; Botta, C.; Borschneck, D.; Sammut, M.; Cabie, M.; Auffan, M.; Rose, J.; Bottero, J.-Y. Aging of TiO_2 Nanocomposites Used in Sunscreen. Dispersion and Fate of the Degradation Products in Aqueous Environment. *Environ. Pollut.* **2010**, *158*, 3482−3489.
(41) Franco-Gil, M. E.; Graça, A.; Martins, A.; Marto, J.; Ribeiro, H. M. Emollients in Dermatological Creams: Early Evaluation for Tailoring Formulation and Therapeutic Performance. *Int. J. Pharm.* **2024**, *653*, 123825.
(42) Sapcharoenkun, C.; Klamchuen, A.; Kasamechonchung, P.; Iemsam-arng, J. Role of Rheological Behavior of Sunscreens Containing Nanoparticles on Thin Film Preparation. *Mater. Sci. Eng., B* **2020**, *259*, 114608.
(43) Calixto, L. S.; Maia Campos, P. M. B. G. Physical-Mechanical Characterization of Cosmetic Formulations and Correlation between Instrumental Measurements and Sensorial Properties. *Int. J. Cosmet. Sci.* **2017**, *39*, 527−534.
(44) Hedjar, L.; Toscani, M.; Gegenfurtner, K. R. Importance of Hue: The Effect of Saturation on Hue-Chroma Asymmetries. *J. Opt. Soc. Am. A* **2025**, *42*, B305−B312.
(45) Braun, G. J.; Fairchild, M. D.; Ebner, F. Color Gamut Mapping in a Hue-Linearized CIELAB Color Space. *Color Imaging Conf.* **1998**, *6*, 163−168.
(46) Bao, W.; Wei, M.; Xiao, K. Investigating Unique Hues at Different Chroma Levels with a Smaller Hue Angle Step. *J. Opt. Soc. Am. A* **2020**, *37*, 671−679.
(47) Wrolstad, R. E.; Smith, D. E. Color Analysis. In *Food Analysis*; Nielsen, S. S., Ed.; Springer US: Boston, MA, 2010; pp 573−586.
(48) Kim, M. H.; Weyrich, T.; Kautz, J. Modeling Human Color Perception under Extended Luminance Levels. *ACM Transactions on Graphics* **2009**, *28*, 27.

https://doi.org/10.1021/acsmaterialslett.5c01351
ACS Materials Lett. XXXX, XXX, XXX−XXX